文章编号:1671-6833(2024)05-0023-07

CT 机双列角接触球转盘轴承建模与振动特性分析

袁 峰[1], 刘凌仲[1], 秦东晨[1], 陈江义[1], 谢兴会[2]

(1.郑州大学 机械与动力工程学院,河南 郑州 450001;2.洛阳 LYC 轴承有限公司,河南 洛阳 471039)

摘 要:为了提高 CT 机主轴承的运转特性,确保 CT 机医学成像的稳定性,以洛阳 LYC 轴承有限公司研制的双列角接触球转盘轴承为研究对象进行建模与振动特性分析。首先,基于 Hertz 接触理论建立轴承在承受复合载荷作用下的力学模型;其次,结合 Newton 运动定律确立轴承外圈 3 自由度非线性动力学微分方程;最后,采用 4 阶 Runge-Kutta 法对微分方程组进行求解,获得轴承外圈的振动特性。在此基础上,通过分析影响轴承振动特性的因素如轴承内、外圈沟曲率半径系数、滚动体数量、游隙、预紧力等,从而确定满足 CT 机主轴承低振动下的最优结构参数。结果表明:轴承振动幅值随着内、外圈沟曲率半径系数的增加呈现出先减小后增大的趋势,将其分别控制在 0.515~0.525、0.510~0.525 更有利于降低轴承的振动;随着滚动体数量的增加,轴承的振动幅值也随之增加,但变化平稳,故在满足设计条件的前提下减少滚动体的数量可以降低轴承振动;随着轴承游隙的增加,轴承的振动幅值先减小后急剧增大,在 18 μm 处振动达到最小;合适的轴向载荷可以有效降低轴承的振动幅值。

关键词:CT 机; 力学模型; 振动模型; 结构参数; 振动加速度

中图分类号:TH133.3;TH113.1 **文献标志码**:A **doi**:10.13705/j.issn.1671-6833.2024.05.007

CT 机主轴承主要用于传递和承受 X 线管、准直仪、探测器、滑环等装置产生的径向载荷和倾覆力矩[1]。由于其运转稳定性直接影响到医学成像的清晰程度,故对于 CT 机主轴承在运行过程中的振动特性也提出了更高的要求。

轴承产生振动的因素[2]是多方面的,包括制造误差、结构振动、运行工况等。陈月等[3]分析了 4 点接触球轴承内外圈圆度误差及阶次对轴承旋转精度的影响。余永健等[4]在考虑轴承内外圈滚道形状误差对轴承回转误差的影响时进一步考虑了轴承零件几何误差引起的滚子-滚道接触位置变化,使得分析模型更加准确、精度更高。余光伟等[5]通过建立 6201 深沟球动力学模型,分析了波纹度波数对轴承振动的影响。吕润楠等[6]在波纹度理论分析的基础上通过 Adams 建立了更加接近轴承实际运行状态下的双列圆锥滚子波纹度动力学模型,分析了波纹度波数对轴承振动的影响。Zmarzy[7]通过测针轮廓仪对轴承表面进行测量,以实验为基础分析了二维、三维轴承表面形貌对振动的影响。汪凯等[8]以 2-DOF 滚动轴承为例分析了游隙对轴承振动特性的研究,但模型未考虑保持架的影响。唐志霖等[9]以压缩机用球轴承为例,综合考虑保持架以及流体动压摩擦力的情况,分析了轴承初始游隙对振动特性的影响。邓四二等[10]、田凯文等[11]分别通过对低噪音深沟球轴承、4 点接触球轴承建立振动数学模型,进一步分析了轴承自身结构参数对其振动加速度值的影响。Parmar 等[12]研究了双列角接触球轴承在承受径向不对中载荷下的振动响应。Gunduz 等[13]以车轮所用的双列角接触球轴承为研究对象分析了轴向、径向预紧力对轴承固有频率和谐振幅的影响。欧旭鹏等[14]基于赫兹接触理论、弹性力学、轴承运动学以及几何学建立了 4 自由度深沟球轴承动力学模型,分析了轴承在受到不平衡扰动力影响下的振动响应机理。Tong 等[15]以圆锥滚子轴承为例,在考虑轴承存在滚子直径误差的情况下,建立了 5 自由度振动数学模型,分析了轴向预紧力以及组合载荷对轴承振动频率的影响。

收稿日期:2024-02-22;**修订日期**:2024-04-09

基金项目:国家重点研发计划项目(2018YFB20005-01);河南省重大科技专项(221100220100)

作者简介:袁峰(1968—),男,河南洛阳人,郑州大学副教授,博士,主要从事机械产品创新设计、工业装配自动化技术方面的研究,E-mail:yuanfeng@zzu.edu.cn。

引用本文:袁峰,刘凌仲,秦东晨,等.CT 机双列角接触球转盘轴承建模与振动特性分析[J].郑州大学学报(工学版),2024,45(5):23-29.(YUAN F,LIU L Z,QIN D C,et al. Modeling and vibration characteristics analysis of double-row angular contact ball turntable bearings in CT machine [J]. Journal of Zhengzhou University(Engineering Science), 2024,45(5):23-29.)

综上所述,有关轴承振动特性的研究主要针对的是小型轴承,而大型转盘轴承主要应用于风电、盾构等重型设备,其工作环境对于轴承的振动特性要求不高,故有关转盘轴承的振动分析很少见。鉴于此,本文针对洛轴研制的双列角接触 CT 机主轴承进行建模和振动特性分析,建立 3 自由度双列角接触球转盘轴承非线性振动模型,采用 4 阶 Runge-Kutta 法对振动微分方程组进行简化求解。通过研究轴承结构参数对振动特性的影响,从而确定出满足 CT 机主轴承低振动下的最优结构参数,为 CT 机主轴承的设计提供一定的理论依据。

1 CT 机主轴承振动数学模型

CT 机双列角接触球转盘轴承的结构示意图如图 1 所示,其中,c_j、K_j、φ_j 分别为第 j 个滚动体处的阻尼、刚度系数和位置角;A 为轴承右端面。本文基于 Hertz 接触理论建立 3 自由度振动数学模型。为便于研究其结构振动特点,特进行如下假设:轴承零部件表面为理想光滑的几何形状;滚动体元素间的接触简化为弹簧和阻尼单元。

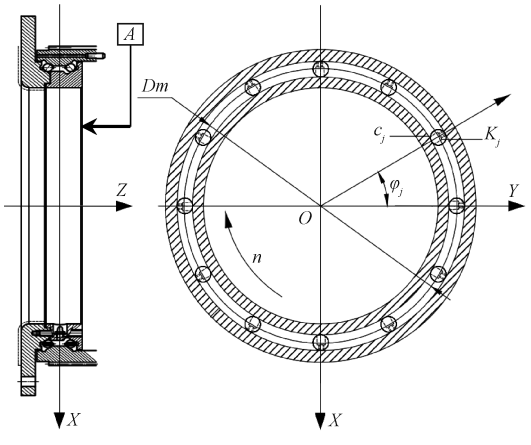

图 1 CT 机主轴承结构示意图

Figure 1 Schematic diagram of the structure of the main bearing of CT machine

1.1 轴承接触刚度与阻尼

1.1.1 等效刚度计算

由 Hertz 接触理论可知,球轴承滚动体和内外滚道接触刚度计算式如下:

$$K_{ki} = 2.15 \times 10^5 \sum \rho_i^{-0.5} (\delta_{ki}^*)^{\frac{3}{2}}; \tag{1}$$

$$K_{ko} = 2.15 \times 10^5 \sum \rho_o^{-0.5} (\delta_{ko}^*)^{\frac{3}{2}}。 \tag{2}$$

式中:$\sum \rho_i$、$\sum \rho_o$ 分别为滚动体与内外圈滚道曲率中心和;δ_{ki}^*、δ_{ko}^* 分别为内外滚道量纲为 1 的接触位移。

1.1.2 等效阻尼计算

阻尼为振动方程不可或缺的一部分。润滑阻尼可以表示为[16]

$$c = \frac{24\pi a \eta_o R^3}{(2Rh_o)^{1.5}}。 \tag{3}$$

式中:a 为钢球与套圈接触区的短半轴长。

由于滚动体在运行过程中与内外圈同时接触,故润滑阻尼为内外圈阻尼复合而成:

$$c = \frac{c_i c_o}{c_i + c_o}。 \tag{4}$$

式中:c_i 表示内圈阻尼;c_o 表示外圈阻尼。

上述阻尼分析为单个滚动体接触时的润滑阻尼,对于整个轴承而言,需要将所有滚动体产生的阻尼进行叠加。方程如下所示:

$$\begin{cases} c_x = c\sum_{j=1}^{z} \cos\alpha_j \cos\dfrac{2\pi(j-1)}{N}; \\ c_y = c\sum_{j=1}^{z} \cos\alpha_j \sin\dfrac{2\pi(j-1)}{N}; \\ c_z = c\sum_{j=1}^{z} \sin\alpha_j。 \end{cases} \tag{5}$$

式中:N 为滚动体的数量;α_j 为接触角。

1.2 CT 机双列角接触球转盘轴承力学模型

由于轴承内圈固定于机架,外圈以 180 r/min 的转速旋转,属于低速运转轴承,因此,力学分析以静力学分析为主。通过上述介绍可知,轴承主要承受 X 线管、准直仪、探测器、滑环等装置产生的复合载荷,其在载荷作用下轴承内外圈会产生相对形变,这种形变等同相应位置的内外圈沟曲率中心的变形。根据轴承运动特点可用 5 个自由度对轴承的运动加以描述,即 $\delta = (\delta_x, \delta_y, \delta_z, \theta_x, \theta_y)$。

如图 2 所示,分别以轴承质心以及两列轴承内圈中心建立坐标系。

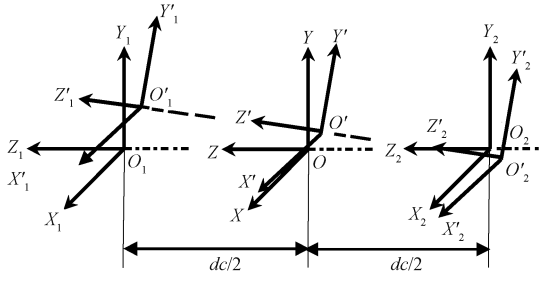

图 2 轴承坐标变换示意图

Figure 2 Schematic diagram of bearing coordinate transformation

由坐标转换原理可得转换矩阵 $\boldsymbol{T}$ 如下所示:

$$\boldsymbol{T}=\begin{bmatrix}\cos\psi\cos\chi & -\cos\psi\sin\chi & \sin\psi\\ \cos\varphi\sin\chi+\sin\varphi\sin\psi\cos\chi & \cos\varphi\cos\chi-\sin\varphi\sin\psi\sin\chi & -\sin\varphi\cos\psi\\ \sin\varphi\sin\chi-\cos\varphi\sin\psi\cos\chi & \sin\varphi\cos\chi+\cos\varphi\sin\psi\sin\chi & \cos\varphi\cos\psi\end{bmatrix}。\tag{6}$$

式中:φ 为 X 轴的旋转角;ψ 为 Y 轴的旋转角;χ 为 Z 轴的旋转角。将 $\varphi=\theta_x$、$\psi=\theta_y$、$\chi=0$ 代入转换矩阵得

$$\boldsymbol{T}=\begin{bmatrix}\cos\theta_y & 0 & \sin\theta_y\\ \sin\theta_x\sin\theta_y & \cos\theta_x & -\sin\theta_x\cos\theta_y\\ -\cos\theta_x\sin\theta_y & \sin\theta_x & \cos\theta_x\cos\theta_y\end{bmatrix}。\tag{7}$$

由坐标变换原理可得轴承受载后坐标系 $O'_1X'_1Y'_1Z'_1$ 相对于 $O_1X_1Y_1Z_1$ 的变换矩阵 $\boldsymbol{T}_1$,如式(8)所示,同理可得轴承受载后坐标系 $O'_2X'_2Y'_2Z'_2$ 相对于 $O_2X_2Y_2Z_2$ 的变换矩阵 $\boldsymbol{T}_2$,如式(9)所示,其中,dc 为两列滚动体的中心距。

$$\boldsymbol{T}_1=\begin{bmatrix}\cos\theta_x & 0 & \sin\theta_y & \delta_x+\frac{dc}{2}\sin\theta_y\\ \sin\theta_x\sin\theta_y & \cos\theta_x & -\sin\theta_x\cos\theta_y & \delta_y-\frac{dc}{2}\sin\theta_x\cos\theta_y\\ -\cos\theta_x\sin\theta_y & \sin\theta_x & \cos\theta_x\cos\theta_y & \delta_z-\frac{dc}{2}+\frac{dc}{2}\cos\theta_x\cos\theta_y\\ 0 & 0 & 0 & 1\end{bmatrix};\tag{8}$$

$$\boldsymbol{T}_2=\begin{bmatrix}\cos\theta_x & 0 & \sin\theta_y & \delta_x-\frac{dc}{2}\sin\theta_y\\ \sin\theta_x\sin\theta_y & \cos\theta_x & -\sin\theta_x\cos\theta_y & \delta_y+\frac{dc}{2}\sin\theta_x\cos\theta_y\\ -\cos\theta_x\sin\theta_y & \sin\theta_x & \cos\theta_x\cos\theta_y & \delta_z+\frac{dc}{2}-\frac{dc}{2}\cos\theta_x\cos\theta_y\\ 0 & 0 & 0 & 1\end{bmatrix}。\tag{9}$$

变形前,第 1 列轴承外圈滚道曲率中心线上一点 P_{j1} 在 $O_1X_1Y_1Z_1$ 坐标系中的坐标为

$$P_{j1}=(R_o\sin\varphi_j,R_o\cos\varphi_j,0,1)。\tag{10}$$

式中:R_o 为轴承外圈沟道曲率中心圆的半径;φ_j 为滚动体所在的位置角。

$$\varphi_j=\omega_c t+\frac{2\pi(k-1)}{N},k=1,2,\cdots N。\tag{11}$$

式中:ω_c 为轴承保持架的角速度。

轴承在受载变形后外圈沟曲率一点 P_{j1} 坐标变化为 $O'_1X'_1Y'_1Z'_1$ 中的 P'_{j1},将 P'_{j1} 坐标转换到 $O_1X_1Y_1Z_1$ 坐标系下:

$$\begin{aligned}P'_{j1}=\boldsymbol{T}_1P_{j1}=&\left(R_o\sin\varphi_j\cos\theta_x+\delta_x+\frac{dc}{2}\sin\theta_y,\right.\\ &R_o\sin\varphi_j\sin\theta_x\sin\theta_y+R_o\cos\varphi_j\cos\theta_x+\delta_y-\\ &\frac{dc}{2}\sin\theta_x\cos\theta_y,-R_o\sin\varphi_j\cos\theta_x\sin\theta_y+R_o\cos\varphi_j\cdot\\ &\left.\sin\theta_x+\delta_z-\frac{dc}{2}+\frac{dc}{2}\cos\theta_x\cos\theta_y,1\right)。\end{aligned}\tag{12}$$

由于接触过程中产生的弹性变形量通常为微小量,因此可取 $\sin\theta=\theta$,$\cos\theta=1$,则在第 j 个滚动体处,滚动体在 XYZ 方向上的弹性变形量:

$$\Delta_{j1}=P'_{\varphi1}-P_{\varphi1}=(\Delta_{x1},\Delta_{y1},\Delta_{z1},0)。\tag{13}$$

考虑轴承游隙,可得滚动体与内外圈在法向上的接触的总变形量为

$$\delta_{j1}=\delta_{\varphi a1}\sin\alpha_{j1}+\delta_{\varphi r1}\cos\alpha_{j1}-C。\tag{14}$$

式中:$\delta_{\varphi a1}=\Delta_{z1}$ 为轴向位移量;$\delta_{\varphi r1}=\Delta_{x1}\sin\varphi_j+\Delta_{y1}\cos\varphi_j$ 为径向位移量;α_{j1} 为轴承接触角;C 为轴承初始游隙。由 Hertz 接触理论可知,双列滚动体第 1 列中第 j 个滚动体处的接触载荷为

$$F_{j1}=K_n\delta_{j1}^{\frac{3}{2}}=K_n(\delta_{\varphi a1}\sin\alpha_{j1}+\delta_{\varphi r1}\cos\alpha_{j1}-C)^{\frac{3}{2}}。\tag{15}$$

同理可得第二列中第 j 个滚动体处的 Hertz 接触应力为

$$F_{j2}=K_n\delta_{j2}^{\frac{3}{2}}=K_n(\delta_{\varphi a2}\sin\alpha_{j2}+\delta_{\varphi r2}\cos\alpha_{j2}-C)^{\frac{3}{2}}。\tag{16}$$

则所有滚动体在各个方向上产生的合力如下。

在 X 轴方向上(径向):

$$F_x=F_{x1}+F_{x2}=\sum_{\psi=0}^{\pm\pi}F_{j1}\cos\alpha_{j1}\cos\varphi_j+\sum_{\psi=0}^{\pm\pi}F_{j2}\cos\alpha_{j2}\cos\varphi_j。\tag{17}$$

在 Z 轴方向上(轴向):

$$F_z=F_{z1}-F_{z2}=\sum_{\psi=0}^{\pm\pi}F_{j1}\sin\alpha_{j1}-\sum_{\psi=0}^{\pm\pi}F_{j2}\sin\alpha_{j2}。\tag{18}$$

绕 Y 轴产生的倾覆力矩:

$$M_y = M_{y1} - M_{y2} = \frac{1}{2}Dm\sum_{\psi=0}^{\pm\pi} F_{j1}\sin\alpha_{j1}\cos\varphi_j - \frac{1}{2}Dm\sum_{\psi=0}^{\pm\pi} F_{j2}\sin\alpha_{j2}\cos\varphi_j。\tag{19}$$

1.3 CT 机双列角接触球转盘轴承振动方程确立

由于轴承在设计之初已经经过动平衡,且其挂载的 X 线管、准直仪、探测器、滑环等装置为圆周分布,故在计算过程中忽略部件自重产生的离心力。如图 1 所示,部件简化质量 m_s 为距 A 端面 283 mm 处施加平行于 X 轴 6 800 N 的径向载荷。简化上述方程,建立 X 轴、Z 轴方向的平动以及 Y 轴方向的转动,则 CT 机双列角接触球转盘轴承 3 自由度非线性振动方程如下所示:

$$\begin{cases} m\ddot{z} + c_z\dot{z} + F_z = 0; \\ m\ddot{x} + c_x\dot{x} + F_x = m_s g; \\ m\ddot{\theta} + c_y\dot{\theta} + M_y = M。 \end{cases}\tag{20}$$

式中:m 为双列角接触球转盘轴承的外圈质量。

2 CT 机主轴承振动特性分析

上述振动方程为二阶非线性微分方程组,本文采用 4 阶 Runge-Kutta 数值方法对其进行求解,得到轴承外圈在各个方向上的振动加速度信号。假设轴承外圈初始位移 $x = z = \theta = 0$;初始速度 $\dot{z} = \dot{x} = \dot{\theta} = 0$,时间间隔 $\Delta t = 0.000\ 1$(采样频率为 10 000 Hz),起始时间 $t_1 = 0.01$ s,结束时间 $t_2 = 0.03$ s。轴承的结构参数如表 1 所示,设定轴承外圈转速为 180 r/min,轴承外圈质量为 46.3 kg,轴承受到的轴向载荷为 0,径向载荷为 6 800 N,倾覆力矩为 2 100 N·m。

表 1 CT 机主轴承结构参数

Table 1 Structural parameters of main bearings of CT machine

参数	取值
轴承外径/mm	1 220
轴承内径/mm	1 002
轴承宽度/mm	96
单列滚动体数量	207
钢球直径/mm	12
初始接触角/(°)	35
内圈沟曲率半径系数	0.554
外圈沟曲率半径系数	0.554

为描述轴承的整体振动水平,本文对振动方程求解后的径向振动数据进行分析,采用轴承振动加速度级 L 对轴承振动水平进行评价[17]:

$$L = 20\lg\frac{a_i}{a_o}。\tag{21}$$

式中:a_i 为振动加速度的均方根值;a_o 为振动标准参考值,其值为 9.81×10^{-3} m/s^2。

2.1 结构参数与工况对轴承振动的影响

图 3 与图 4 分别为 CT 机主轴承在径向载荷为 6 800 N,倾覆力矩为 2 100 N·m 时,各参数与工况

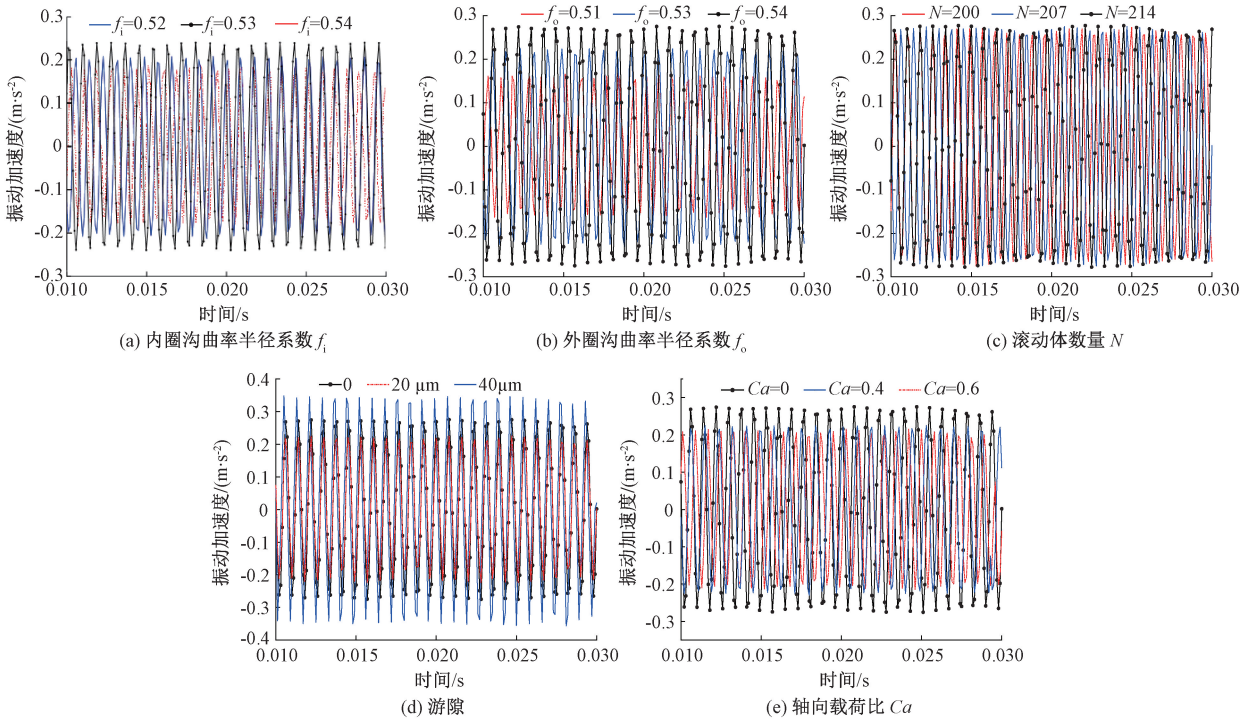

(a) 内圈沟曲率半径系数 f_i (b) 外圈沟曲率半径系数 f_o (c) 滚动体数量 N

(d) 游隙 (e) 轴向载荷比 Ca

图 3 各参数对轴承振动加速度的影响

Figure 3 Influence of each parameter on the vibration acceleration of the bearing

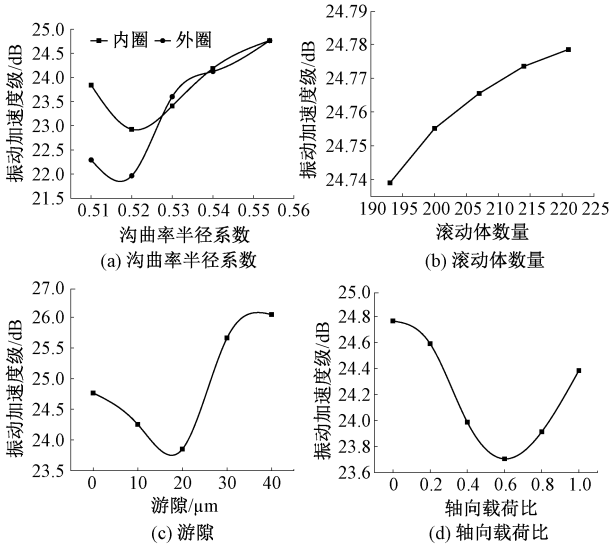

图 4　各参数对轴承振动加速度级的影响

Figure 4　Influence of each parameter bearing on the vibration acceleration level of the bearing

对轴承振动加速度与振动级的影响。

2.1.1　内圈沟曲率半径系数对轴承振动的影响

从图 4(a)可以看出,随着内圈沟曲率的增加,轴承的振动呈现先减小后增加的趋势,且在沟曲率为 0.522 附近振动达到最小。故在选取轴承内圈沟曲率半径系数时,将其控制在 0.515~0.525 更有利于降低轴承的振动。

2.1.2　外圈沟曲率半径系数对轴承振动的影响

从图 4(a)可以看出,随着外圈沟曲率的增加,轴承振动趋势和内圈沟曲率变化趋势一致,表现为先减小后增大且在曲率为 0.518 附近达到最小。故在选取轴承外圈沟曲率半径系数时将其控制在 0.510~0.525 更有利于降低轴承的振动。

2.1.3　滚动体数量对轴承振动的影响

从图 4(b)可知,随着滚动体数量的增加,轴承振动趋势也随之增加,但其总体振动幅值变化平稳,无剧烈变化。滚动体数量增加虽然降低了单个滚动体承载的载荷,但也增加了振动源。从振动角度分析,减小滚动体的数量有利于降低轴承的振动。故在轴承设计之初,在满足轴承的承载能力条件下可以减少滚动体的数量从而降低振动,但降低的幅值有限。

2.1.4　游隙对轴承振动的影响

由图 4(c)可知,随着游隙的增加,轴承的振动先减小后急剧增大,在 18 μm 处达到最小,且当轴承游隙大于 20 μm 后,轴承振动幅值随着游隙的增加而增加。这主要是由于当轴承游隙过小时,游隙限制了滚动体在交替受载过程中的相对位移能力,导致振动无法得到充分缓解,从而使振动幅值增加,且当游隙过小时无法形成有效润滑从而增加轴承的摩擦与磨损。而当轴承游隙过大时,会引起滚动体与内外圈的剧烈碰撞,造成振动的急剧增加,故轴承游隙应控制在 18 μm 附近。

2.1.5　轴向载荷对轴承振动的影响

轴向载荷比 Ca 定义为轴承轴向载荷与径向载荷之比:$Ca=Fa/Fr$。从图 4(d)可以看出,随着轴向力的增加,轴承的振动幅值呈现先减小后增加的趋势,在轴向载荷比 0.6 附近时,振动幅值达到最小。故对轴承施加合适的轴向载荷可以有效降低轴承的振动幅值。

3　结论

(1)通过 Hertz 接触理论建立了 CT 机双列角接触球转盘力学模型,并进一步对其非线性振动模型进行分析。

(2)通过对 CT 机双列角接触球转盘轴承振动模型分析,发现存在最优的结构参数使得轴承的振动降低。如减少滚动体的数量,将轴承内圈沟曲率控制在 0.515~0.525,外圈沟曲率控制在 0.510~0.525,游隙控制在 18 μm 附近。

(3)轴承在运行过程中存在合适的轴向载荷使得轴承振动降低,因此可通过两内圈相连的螺栓对轴承进行一定的预紧从而降低轴承的振动。

参考文献:

[1] 温景波, 周琳, 谢兴会, 等. 高速 CT 机主轴承[J]. 轴承, 2012(9): 9-10.
WEN J B, ZHOU L, XIE X H, et al. Main bearing of high-speed CT[J]. Bearing, 2012(9): 9-10.

[2] 梁杰, 张志强, 高金刚. 40Cr/石墨关节轴承摩擦学性能及磨损机理研究[J]. 郑州大学学报(工学版), 2022, 43(2): 65-70.
LIANG J, ZHANG Z Q, GAO J G. Study on tribological properties and wear mechanism of 40Cr/graphite spherical plain bearings[J]. Journal of Zhengzhou University (Engineering Science), 2022, 43(2): 65-70.

[3] 陈月, 邱明, 杜辉, 等. 机器人用四点接触球轴承旋转精度影响因素[J]. 中国机械工程, 2020, 31(14): 1678-1685, 1692.
CHEN Y, QIU M, DU H, et al. Factors influencing rotation accuracy of four-point contact ball bearings for robots [J]. China Mechanical Engineering, 2020, 31(14): 1678-1685, 1692.

[4] 余永健, 陈国定, 李济顺, 等. 轴承零件几何误差对圆柱滚子轴承回转误差的影响: 第一部分 计算方法[J]. 机械工程学报, 2019, 55(1): 62-71.
YU Y J, CHEN G D, LI J S, et al. Effect of geometric

errors of bearing components on motion error of cylindrical roller bearings: part Ⅰ calculation method[J]. Journal of Mechanical Engineering, 2019, 55(1): 62-71.

[5] 余光伟, 方党生, 蔡翔宇, 等. 波纹度波数对深沟球轴承振动特性的影响[J]. 轴承, 2021(4): 18-22.
YU G W, FANG D S, CAI X Y, et al. Influence of waviness wave number on vibration characteristics of deep groove ball bearing[J]. Bearing, 2021(4): 18-22.

[6] 吕润楠, 郝旭, 于长鑫, 等. 双列圆锥滚子轴承滚道表面波纹度对轴承振动特性的影响研究[J]. 振动与冲击, 2022, 41(20): 126-132.
LYU R N, HAO X, YU C X, et al. Effects of vibration characteristics of a double row tapered roller bearing with raceway surface waviness[J]. Journal of Vibration and Shock, 2022, 41(20): 126-132.

[7] ZMARZY P . Influence of bearing raceway surface topography on the level of generated vibration as an example of operational heredity[J]. Indian Journal of Engineering and Materials Sciences, 2020, 27(2):356-364.

[8] 汪凯, 江胜飞, 胡波, 等. 轴承间隙对轴承振动影响的理论模型与试验研究[J]. 机械科学与技术, 2023, 42(1): 67-74.
WANG K, JIANG S F, HU B, et al. Theoretical model and experimental study on influence of bearing inner clearance on bearing vibration[J]. Mechanical Science and Technology for Aerospace Engineering, 2023, 42(1): 67-74.

[9] 唐志霖, 蒋迪永, 张文虎, 等. 时变载荷激励的空调滑片式压缩机用球轴承振动特性分析[J]. 振动与冲击, 2023, 42(1): 169-180, 223.
TANG Z L, JIANG D Y, ZHANG W H, et al. Vibration characteristics of ball bearing for air conditioning sliding vane compressor excited by time-varying load[J]. Journal of Vibration and Shock, 2023, 42(1): 169-180, 223.

[10] 邓四二, 孙朝阳, 顾金芳, 等. 低噪音深沟球轴承振动特性研究[J]. 振动与冲击, 2015, 34(10): 12-19.
DENG S E, SUN C Y, GU J F, et al. Vibration characteristics of low-noise deep groove ball bearings[J]. Journal of Vibration and Shock, 2015, 34(10): 12-19.

[11] 田凯文, 邱明, 王东峰. 动力传动机构四点接触球轴承的振动特性分析[J]. 振动与冲击, 2023, 42(4): 39-47.
TIAN K W, QIU M, WANG D F. Analysis of vibration characteristics of four-point contact ball bearings for power transmission[J]. Journal of Vibration and Shock, 2023, 42(4): 39-47.

[12] PARMAR V, SARAN V H, HARSHA S P. Effect of dynamic misalignment on the vibration response, trajectory followed and defect-depth achieved by the rolling-elements in a double-row spherical rolling-element bearing[J]. Mechanism and Machine Theory, 2021, 162: 104366.

[13] GUNDUZ A, DREYER J T, SINGH R. Effect of bearing preloads on the modal characteristics of a shaft-bearing assembly: experiments on double row angular contact ball bearings[J]. Mechanical Systems and Signal Processing, 2012, 31: 176-195.

[14] 欧旭鹏, 张义民, 张凯, 等. 考虑不平衡力与扰动力的深沟球轴承动力学模型[J]. 机械设计与制造, 2022(12): 6-10.
OU X P, ZHANG Y M, ZHANG K, et al. Dynamic model of deep groove bearing considering unbalanced force and disturbing force[J]. Machinery Design & Manufacture, 2022(12): 6-10.

[15] TONG V C, HONG S W. Vibration characteristics of tapered roller bearings with roller diameter error[J]. MATEC Web of Conferences, 2016, 51: 01004.

[16] 杜秋华. 球轴承振动的非线性模型及信号分析方法研究[D]. 武汉: 华中科技大学, 2007.
DU Q H. Research on nonlinear models and signal analysis methods of ball bearing vibrations[D]. Wuhan: Huazhong University of Science and Technology, 2007.

[17] 中华人民共和国工业和信息化部. 滚动轴承振动(加速度)测量方法:JB/T 5314—2013[S]. 北京:机械工业出版社,2013.
Ministry of Industry and Information Technology of the People's Republic of China. Rolling bearing vibration (acceleration) measurement method: JB/T 5314—2013[S]. Beijing:China Machine Press,2013.

Modeling and Vibration Characteristics Analysis of Double-row Angular Contact Ball Turntable Bearings in CT Machine

YUAN Feng[1], LIU Lingzhong[1], QIN Dongchen[1], CHEN Jiangyi[1], XIE Xinghui[2]

(1. School of Mechanical and Power Engineering, Zhengzhou University, Zhengzhou 450001, China; 2. Luoyang LYC Bearing Co., Ltd., Luoyang 471039, China)

Abstract: In order to improve the running characteristics of the main bearing of the CT machine and ensure the stability of the medical imaging of the CT machine, the double-row angular contact ball turntable bearing developed by

Luoyang LYC Bearing Co., Ltd. was used as the research object for modeling and vibration characteristic analysis. Firstly, based on Hertz's contact theory, the mechanical model of the bearing with the action of composite load was established. Then the nonlinear dynamic differential equation of the bearing outer ring with 3 degrees of freedom was established in combination with Newton's law of motion. Finally the differential equation system was solved by the fourth-order Runge-Kutta method to obtain the vibration characteristics of the bearing outer ring. On this basis, by analyzing the factors affecting the vibration characteristics of the bearing, such as the radius coefficient of curvature of the groove in the inner and outer rings of the bearing, the number of rolling elements, the clearance, the preload, etc., the optimal structural parameters to meet the low vibration of the main bearing of the CT machine were determined. The results show that the vibration amplitude of the bearing decreases first and then increases with the increase of the radius coefficient of curvature of the inner and outer ring grooves, which were controlled at 0.515 to 0.525, respectively. The range of 0.510 to 0.525 was more conducive to reducing the vibration of the bearing. With the increase of the number of rolling elements, the vibration amplitude of the bearing also increases, but the change was stable, so the vibration of the bearing can be reduced by reducing the number of rolling elements under the premise of satisfying the design conditions. With the increase of the bearing clearance, the vibration amplitude of the bearing decreases first and then increases sharply, and the vibration reaches the minimum at 18 μm. Appropriate axial load can effectively reduce the vibration amplitude of the bearing.

Keywords: CT machine; mechanical model; vibration model; structural parameter; vibration acceleration

(上接第 15 页)

Adaptive Variable Gain Transmission Ratio Design for Automotive Steer-by-wire Systems

KOU Farong, FANG Bo, ZHANG Xinqian, CHANG Hangtao

(School of Mechanical Engineering, Xi'an University of Science and Technology, Xi'an 710054, China)

Abstract: The variable steering transmission ratio was a crucial factor affecting the active safety and handling stability of vehicles. In order to enhance the steering characteristics of steering-by-wire vehicles on low-adhesion coefficient road surfaces, a variable gain transmission ratio that adapts to changes in road adhesion coefficient and vehicle speed was designed. A 2 DOF model was established for the vehicle, to analyze the factors influencing the yaw rate gain, and to obtain the data relationship between the influencing factors and the gain through simulation. The Min-Max normalization method was utilized to preprocess the data between the influencing factors and the yaw rate gain, constructing a neural network dataset. Design a Snake Optimizer Backpropagation Neural Network (SO-BP) was desighed and train to use the preprocessed dataset to dynamically acquire the variable yaw rate gain. A strategy was employed to combines the variable yaw rate gain with the lateral acceleration gain in proportion to design the variable gain transmission ratio for electronic control steering. Simulink-CarSim was used to build a steer-by-wire steering whole vehicle model. Compare and analyze the designed variable gain transmission ratio was analized and compared with a traditional fixed gain transmission ratio under conditions of both high-adhesion coefficient road surfaces with a double lane change scenario and low-adhesion coefficient road surfaces with a step input scenario. Results indicated that with high-adhesion coefficient road conditions, the trajectory error of the two transmission ratio vehicles remained within 3%, while the variable gain transmission ratio vehicle reduced the peak steering wheel angle by 9.1%. With low-adhesion coefficient road conditions, the variable gain transmission ratio vehicle showed a 22.3% reduction in steady-state yaw rate at low to moderate speeds and a 24.6% reduction in peak yaw rate. At moderate to high speeds, the steady-state yaw rate decreased by 6.6%, and the peak yaw rate decreased by 10.8%. The variable gain transmission ratio not only enhanced steering sensitivity on high-adhesion coefficient road surfaces, but also improved safety and maneuverability when driving on low-adhesion coefficient road surfaces.

Keywords: steer-by-wire; yaw rate gain; variable transmission ratio; SO-BP neural network; friction coefficient